

# SUPPORTING INFORMATION:

## Understanding liquid-liquid equilibria in binary mixtures of hydrocarbons with a thermally robust perarylphosphonium-based ionic liquid.

Santosh R. P. Bandlamudi,<sup>a</sup> Jimmie L. McGehee,<sup>a</sup> Albaraa D. Mando,<sup>a</sup>  
Mohammad Soltani,<sup>b</sup> C. Heath Turner,<sup>c</sup> James H. Davis Jr.,<sup>b</sup> Kevin N.  
West,<sup>a</sup> and Brooks D. Rabideau<sup>\*a</sup>

<sup>a</sup> *Department of Chemical & Biomolecular Engineering, The University of South Alabama, Mobile, Alabama 36688, USA.*

<sup>b</sup> *Department of Chemistry, The University of South Alabama, Mobile, Alabama 36688, USA.*

<sup>c</sup> *Department of Chemical & Biological Engineering, The University Alabama, Tuscaloosa, Alabama 35487, USA.*

---

\* Fax: (251) 461-1485; Tel: (251) 460-7147; E-mail: [brabideau@southalabama.edu](mailto:brabideau@southalabama.edu)

# 1 Miscibility Studies

Resultant miscibility profiles for all six simulations discussed in the *Model Validation* section of the main manuscript are provided in Figure S1.

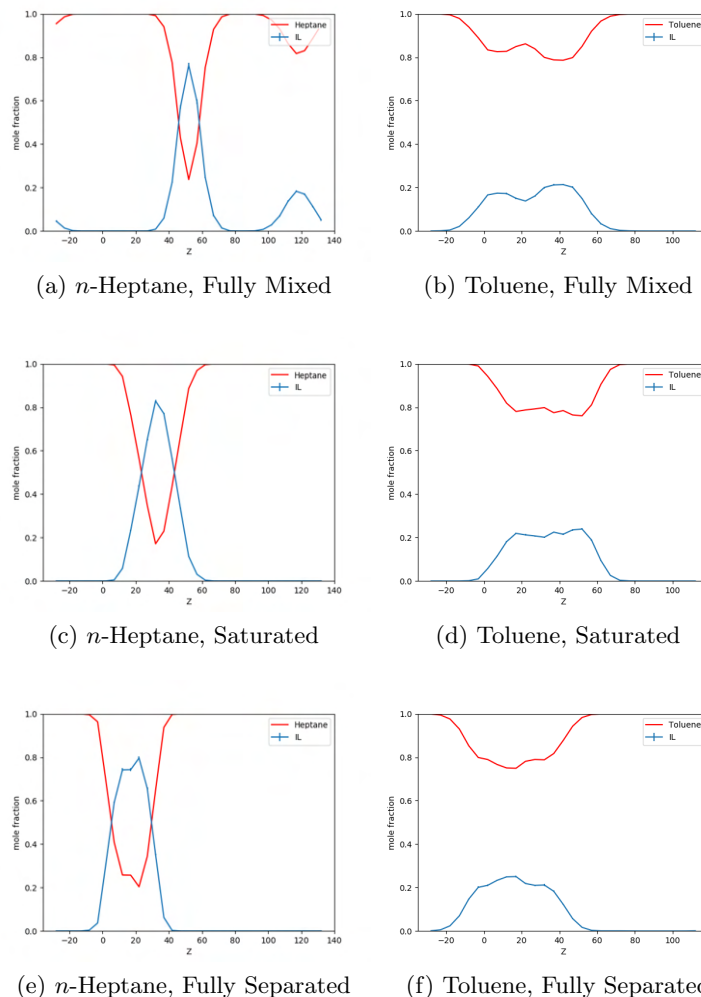


Figure S1: Resultant miscibility profiles for each of the six simulations of the Model Validation section, averaged along the  $Z$ -axis over the last 30 ns of the simulation. For each of the IL-heptane and IL-toluene systems, three separate simulations were performed in an initially fully mixed state, an initially saturated state (84 mol% hydrocarbon), and an initially fully separated state.

Resultant miscibility profiles for all compounds are provided in Figure S2.

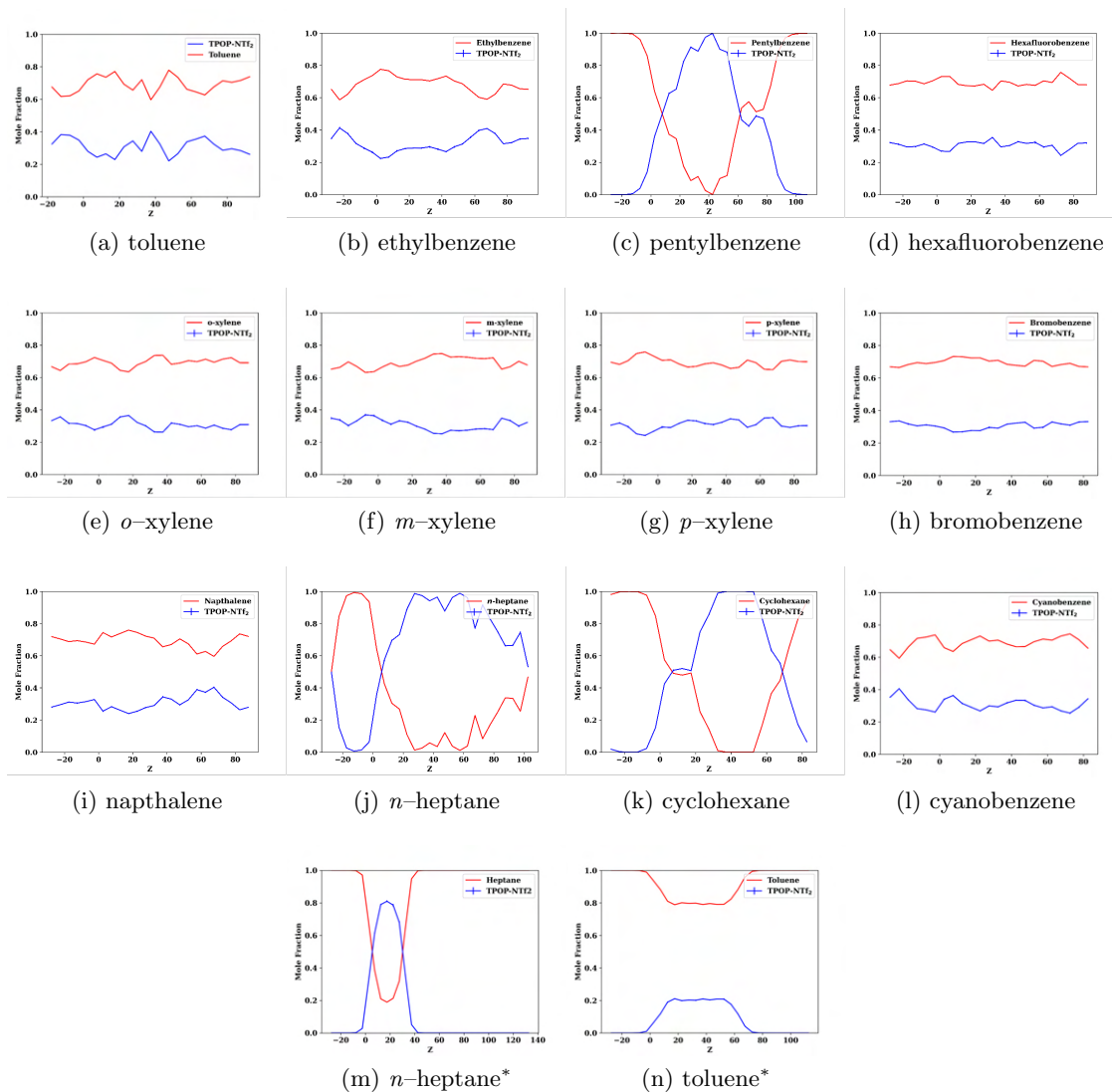


Figure S2: Resultant miscibility profiles for all compounds, averaged along the  $Z$ -axis over the last 30 ns of the 186 ns simulation. Figures marked with an asterisk indicate the simulations of the *Model Validation* section of the main manuscript.

The standard deviations and standard uncertainties for each of these miscibility profiles are provided in Figure S3 and Figure S4, respectively.

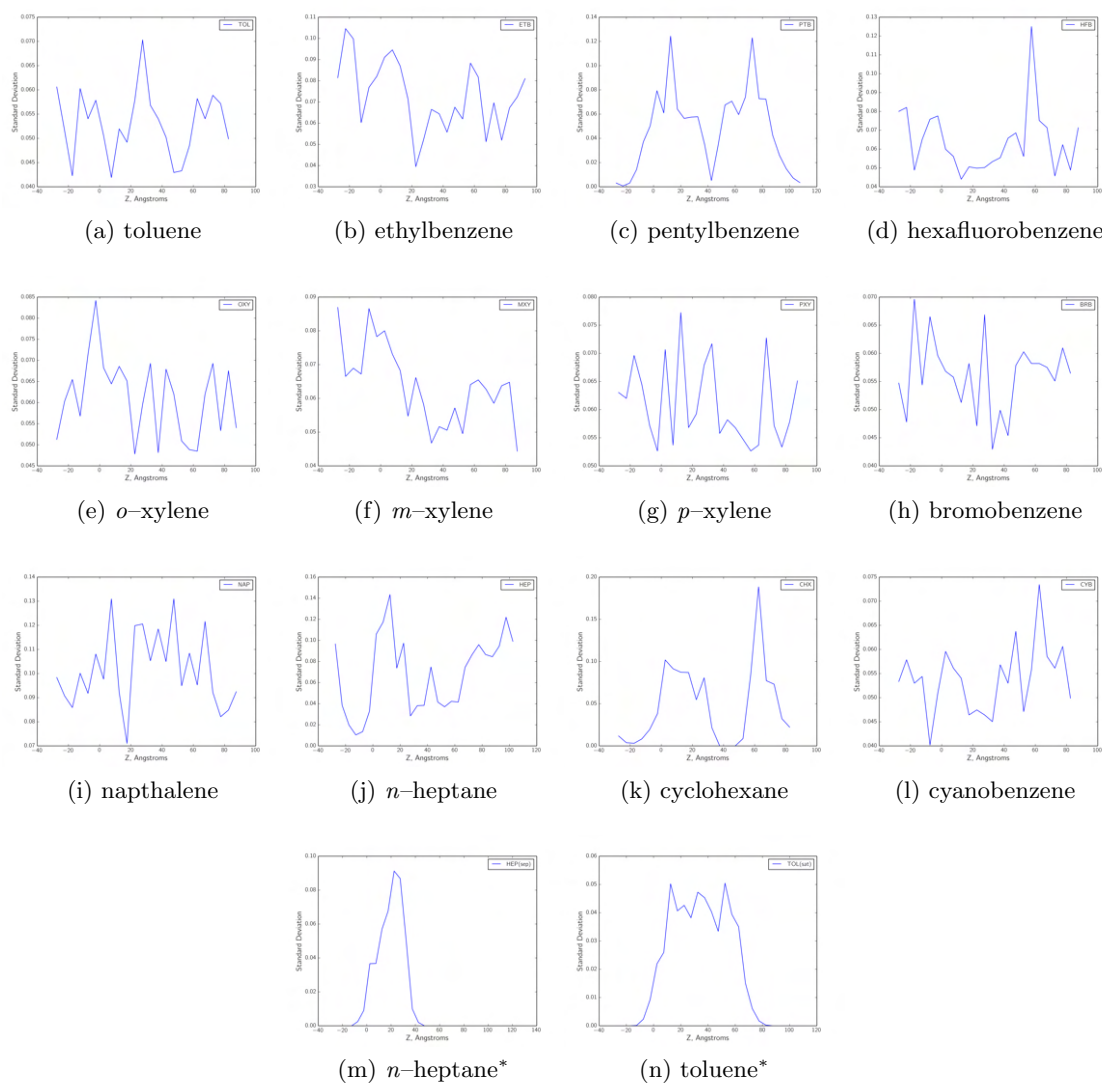


Figure S3: Corresponding standard deviations of the miscibility profiles, along the  $Z$ -axis over the last 30 ns of the 186 ns simulation. Figures marked with an asterisk indicate the simulations of the Model Validation section of the main manuscript.

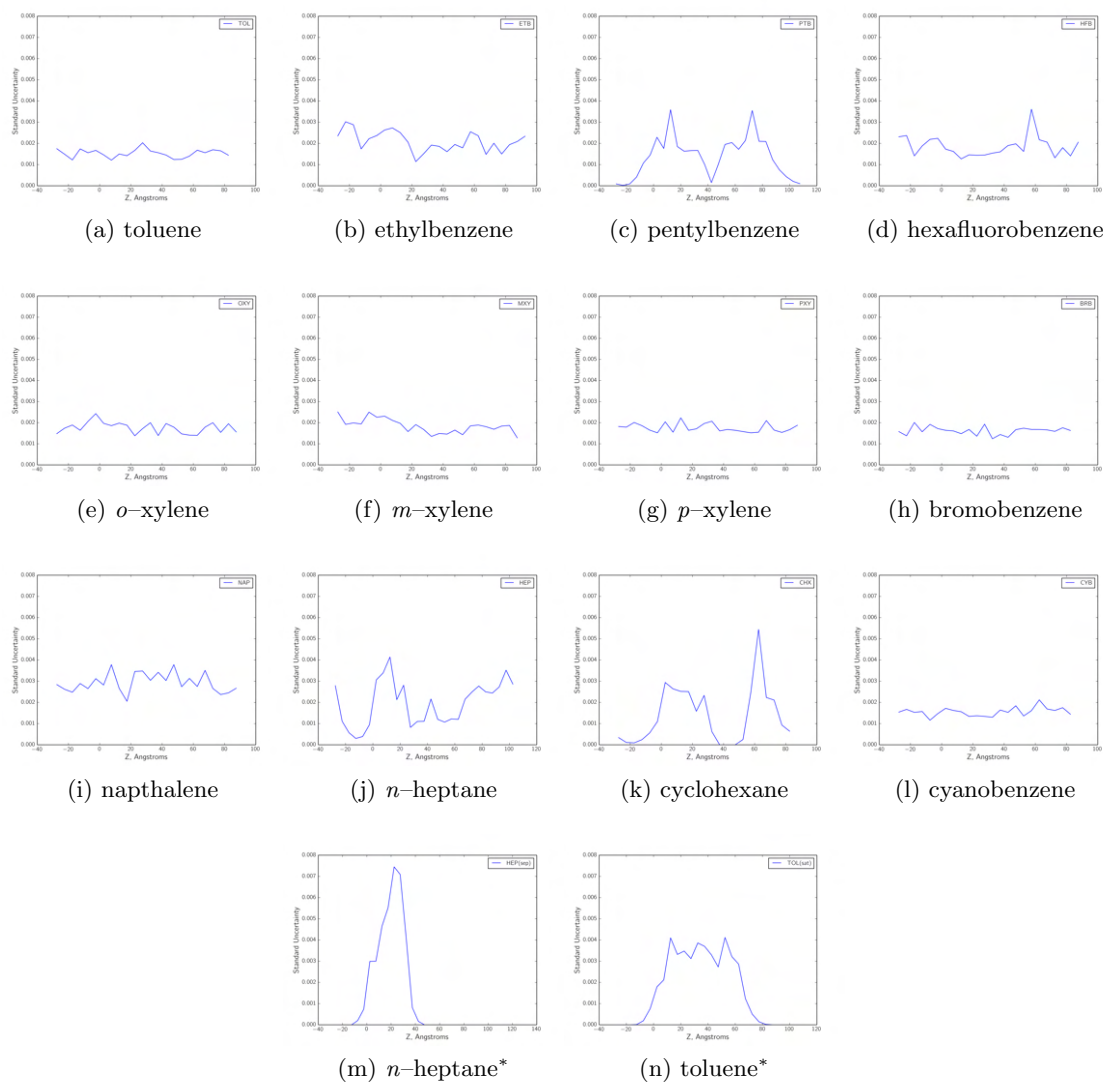


Figure S4: Corresponding standard uncertainties of the miscibility profiles, along the  $Z$ -axis over the last 30 ns of the 186 ns simulation. Figures marked with an asterisk indicate the simulations of the Model Validation section of the main manuscript.

## 2 Radial Distribution Functions

Site-site radial distribution functions between the centers of mass of the hydrocarbons in the neat and ion-rich phase are provided in Figure S5.

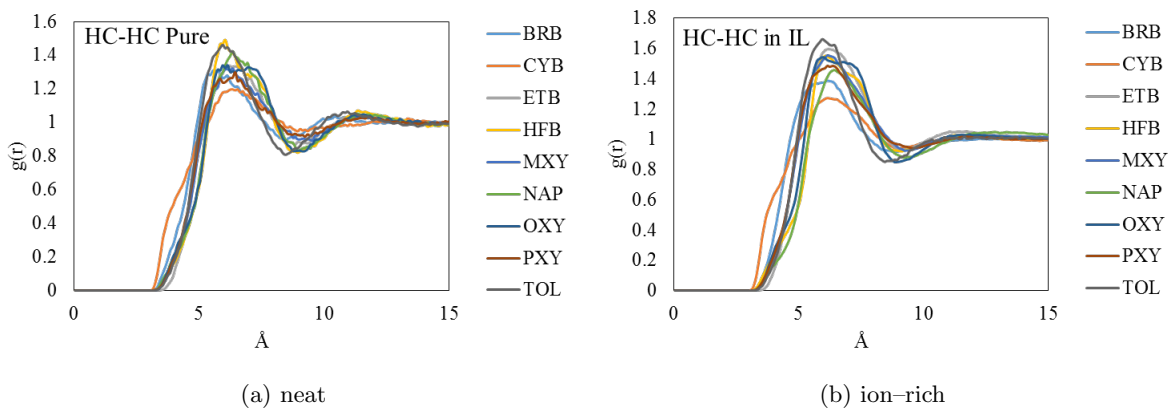


Figure S5: Site-site radial distribution functions between the centers of mass of the hydrocarbons in the (a) neat and (b) ion-rich phase.

### 3 Volume Change on Mixing

Changes in volume upon mixing are presented for each of the systems in Table S1. The reported values

Table S1: Changes in volume of each hydrocarbon–IL system, during the miscibility studies along with estimated standard deviation  $\sigma$  and standard uncertainty  $u_c$ . Values given per mole IL-pair.

System	$\langle \Delta V \rangle$ (cm <sup>3</sup> /mol)	$\sigma$ (cm <sup>3</sup> /mol)	$u_c$ (cm <sup>3</sup> /mol)
Toluene	14.7	3.5	0.6
Ethylbenzene	-11.67	3.23	0.10
Pentylbenzene	12.09	3.28	0.11
<i>o</i> -Xylene	-1.0	3.6	0.5
<i>m</i> -Xylene	4.5	3.0	0.4
<i>p</i> -Xylene	-5.1	2.7	0.5
Napthalene	3.2	3.1	0.3
<i>n</i> -Heptane	-2.19	4.03	0.09
Cyclohexane	4.03	2.36	0.09
Hexafluorobenzene	10.71	3.32	0.10
Bromobenzene	8.4	3.1	0.6
Cyanobenzene	4.2	2.2	0.4

should be interpreted as estimates of the volume change on mixing, as they were determined from the initial and final stages of the dynamic simulations. More specifically, the average volume change on mixing,  $\langle \Delta V \rangle$ , was calculated to be the difference between the average, combined system volume during the first 1-6 ns of the simulation,  $\langle V_{initial} \rangle$ , and the average, combined system volume during the final 5 ns of the simulation,  $\langle V_{final} \rangle$ :

$$\langle \Delta V \rangle = \langle V_{final} \rangle - \langle V_{initial} \rangle.$$

Since each simulation began as two neat phases in contact, the period from 1-6 ns corresponds to period when both systems had achieved a quasi-mechanical equilibrium before the diffusive processes were able to occur. Visual inspection of each of the trajectories confirmed almost no mixing of the phases during this initial short time period.

## 4 Spatial Distribution Functions

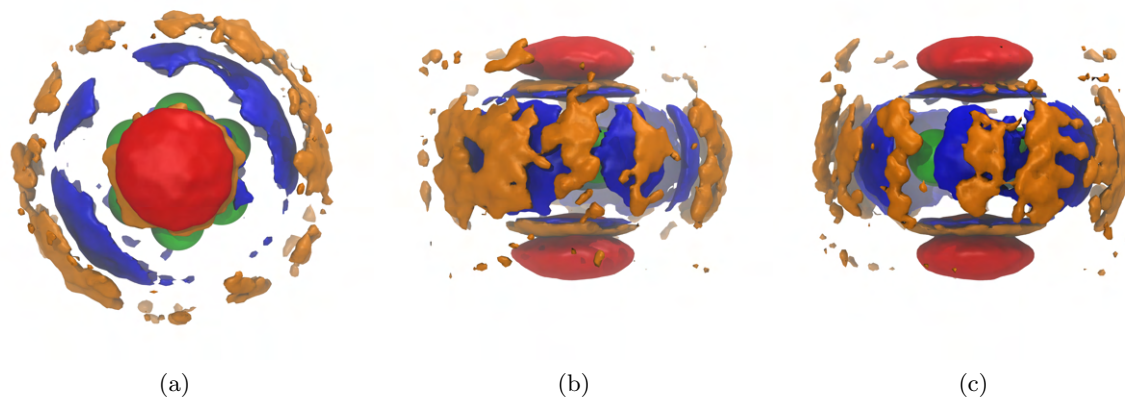


Figure S6: Spatial distribution functions around (a-c) perfluorobenzene (red,  $1.75\times$ ) the nitrogen of the anion, (blue,  $2.3\times$ ) center of mass of neighboring solutes, and (orange,  $1.15\times$ ) the phosphorous atom of neighboring cations. Left, middle, and right figures show top-down views, front views, and side views, respectively.



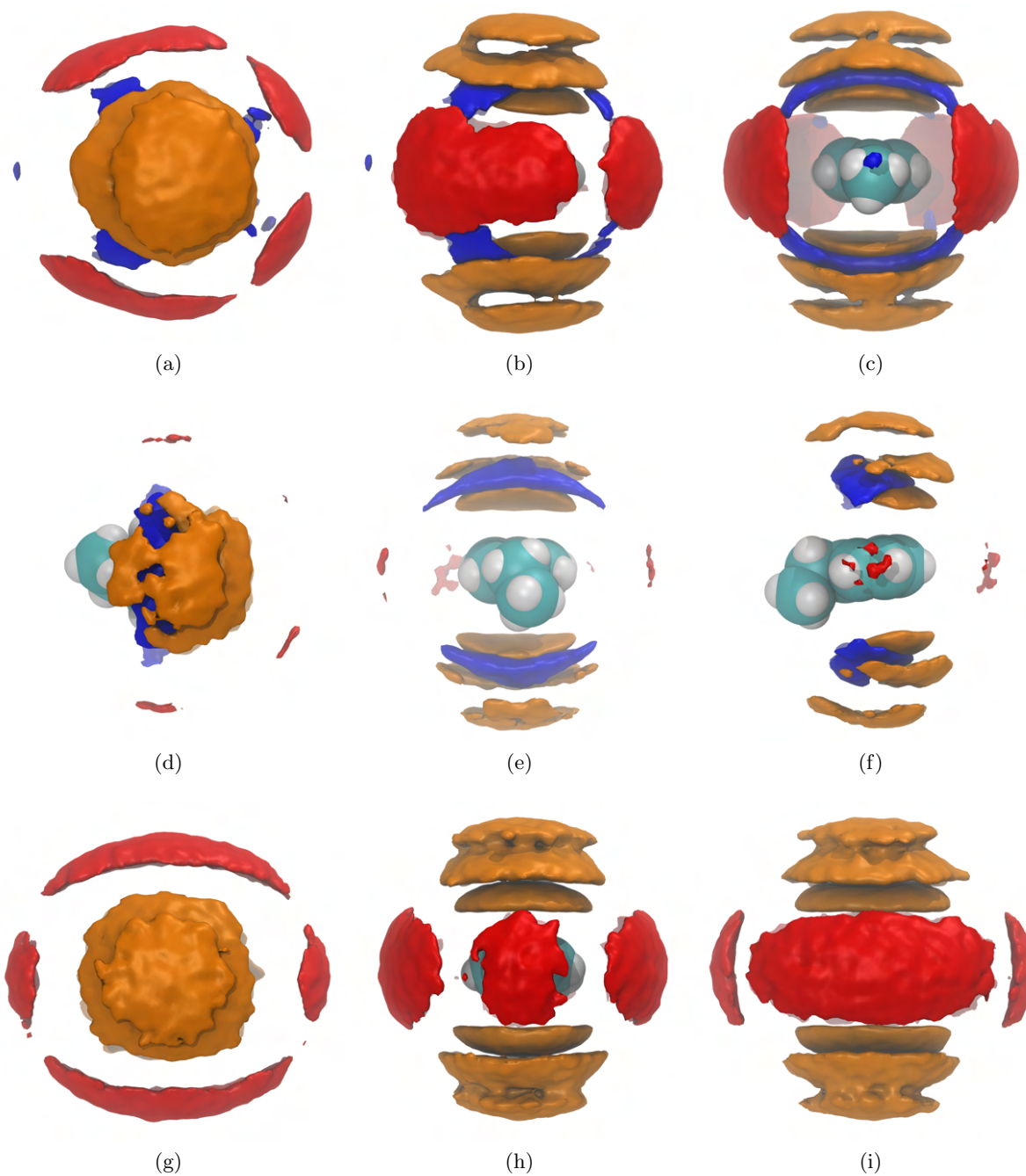


Figure S7: Spatial distribution functions around (a-c) toluene, (d-f) ethylbenzene, and (g-i) naphthalene showing (red,  $1.75\times$ ) the nitrogen of the anion, (blue,  $3.5\times$ ) center of mass of neighboring solutes, and (orange,  $1.25\times$ ) the phosphorous atom of neighboring cations. Left, middle, and right figures show top-down views, front views, and side views, respectively.

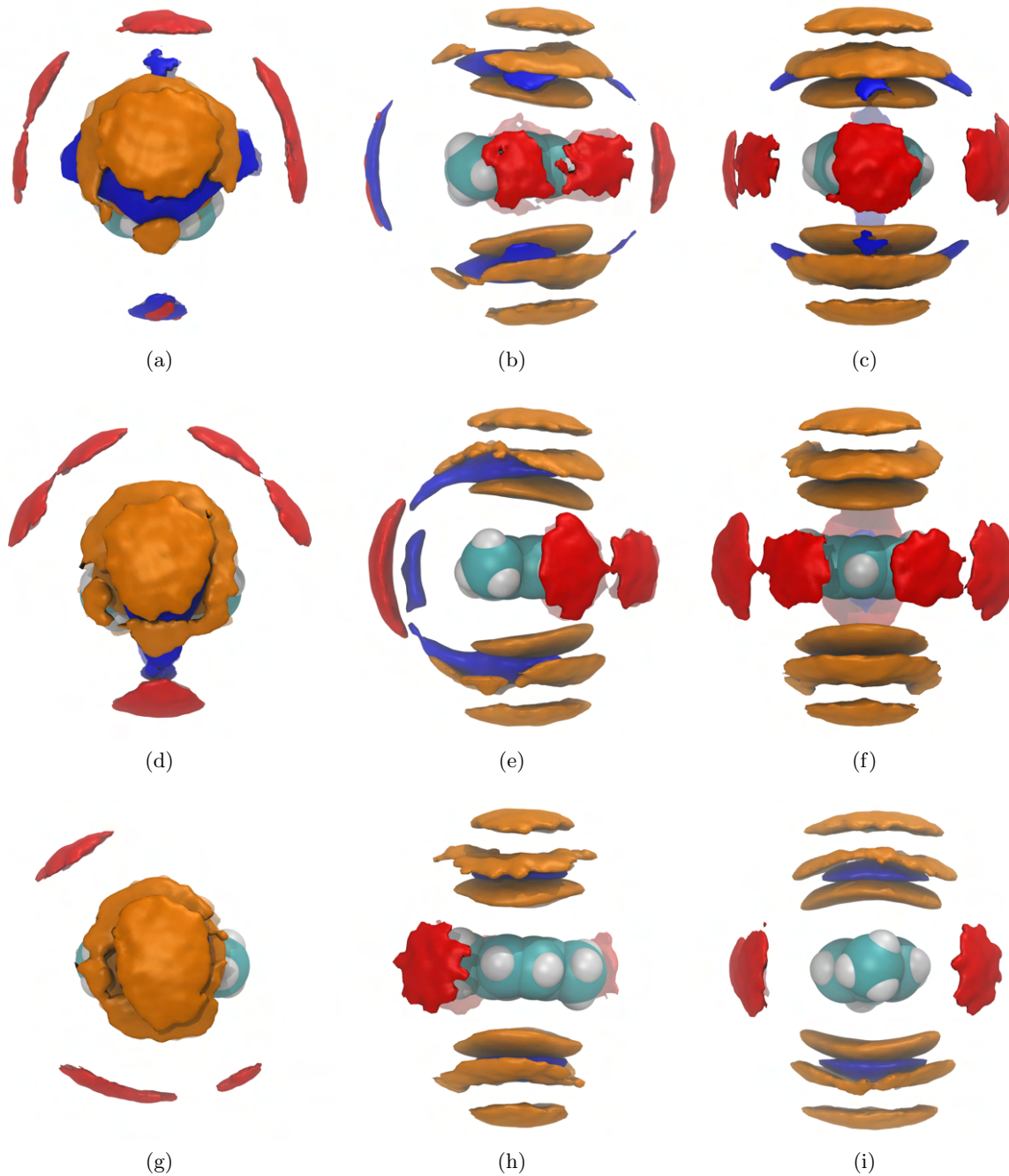


Figure S8: Spatial distribution functions around (a-c) *o*-xylene, (d-f) *m*-xylene, and (g-i) *p*-xylene (red,  $1.75\times$ ) the nitrogen of the anion, (blue,  $3.5\times$ ) center of mass of neighboring solutes, and (orange,  $1.25\times$ ) the phosphorous atom of neighboring cations. Left, middle, and right figures show top-down views, front views, and side views, respectively.

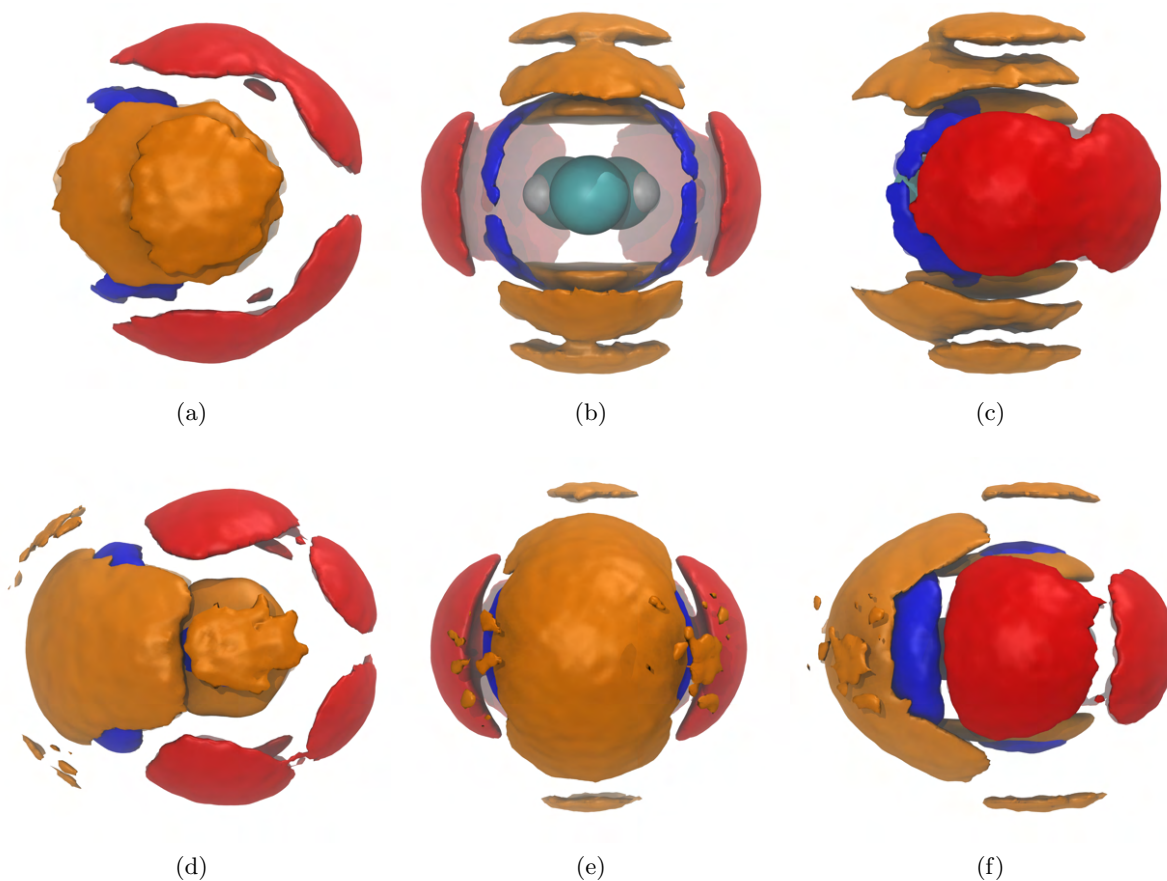


Figure S9: Spatial distribution functions around (a-c) bromobenzene and (d-f) cyanobenzene showing (red,  $1.75\times$ ) the nitrogen of the anion, (blue,  $3.5\times$ ) center of mass of neighboring solutes, and (orange,  $1.25\times$ ) the phosphorous atom of neighboring cations. Left, middle, and right figures show top-down views, front views, and side views, respectively.

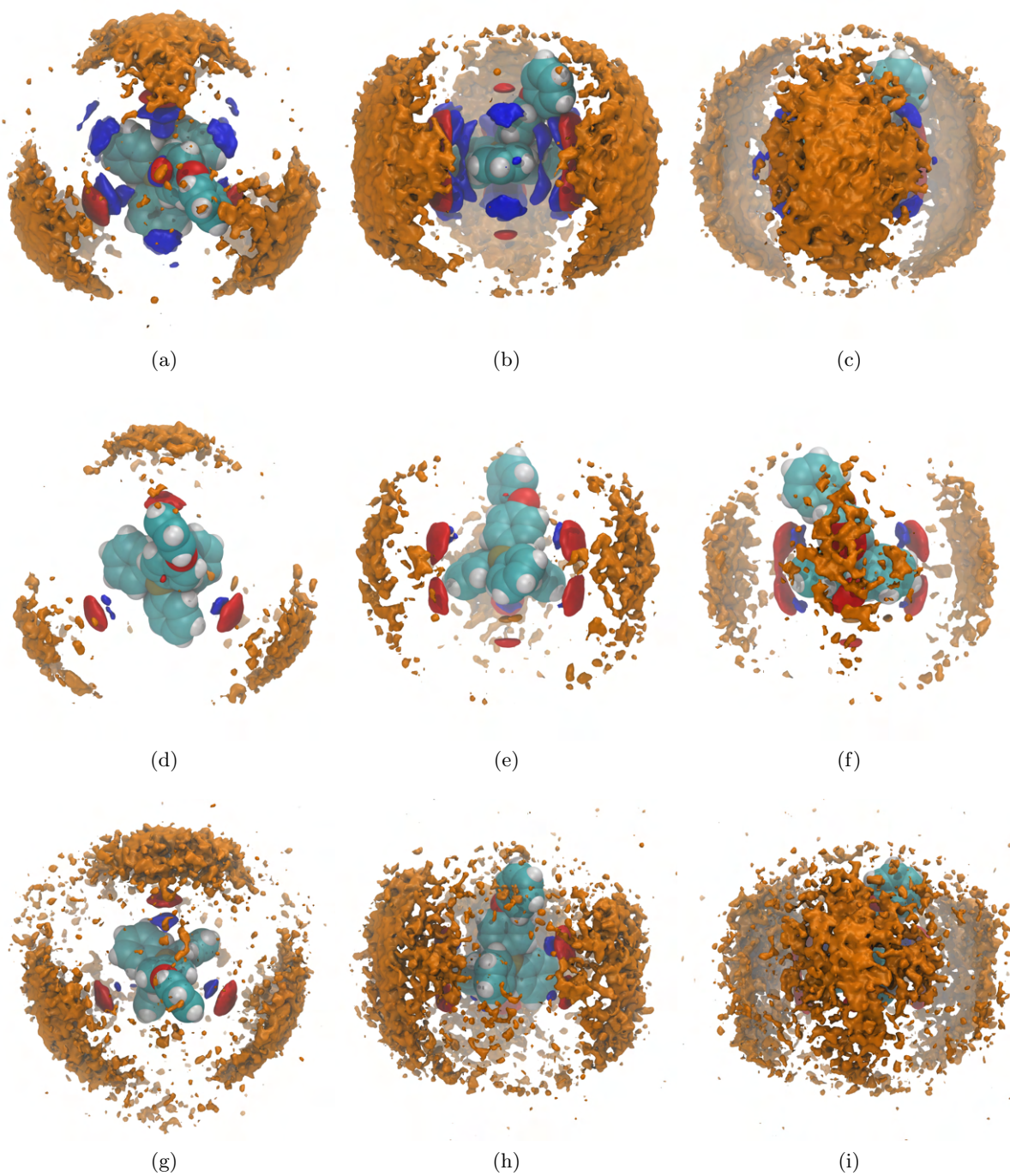


Figure S10: Spatial distribution functions around cations with (a-c) toluene, (d-f) ethylbenzene, and (g-i) naphthalene showing (red,  $3\times$ ) the nitrogen of the anion, (blue,  $3\times$ ) center of mass of neighboring solutes, and (orange,  $1\times$ ) the phosphorous atom of neighboring cations. Left, middle, and right figures show top-down views, front views, and side views, respectively.

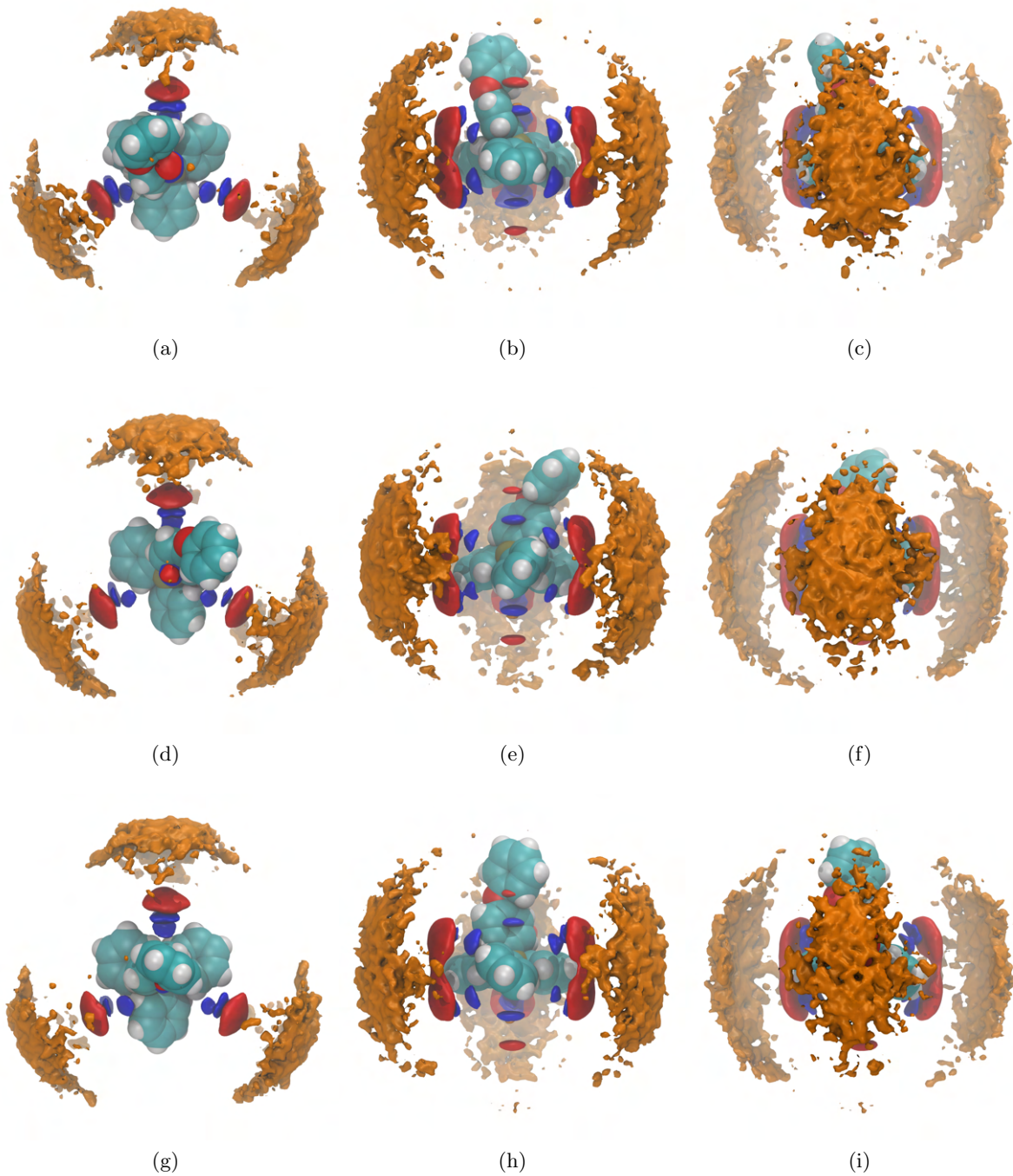


Figure S11: Spatial distribution functions around cations with (a-c) *o*-xylene, (d-f) *m*-xylene, and (g-i) *p*-xylene showing (red,  $3\times$ ) the nitrogen of the anion, (blue,  $3\times$ ) center of mass of neighboring solutes, and (orange,  $1\times$ ) the phosphorous atom of neighboring cations. Left, middle, and right figures show top-down views, front views, and side views, respectively.

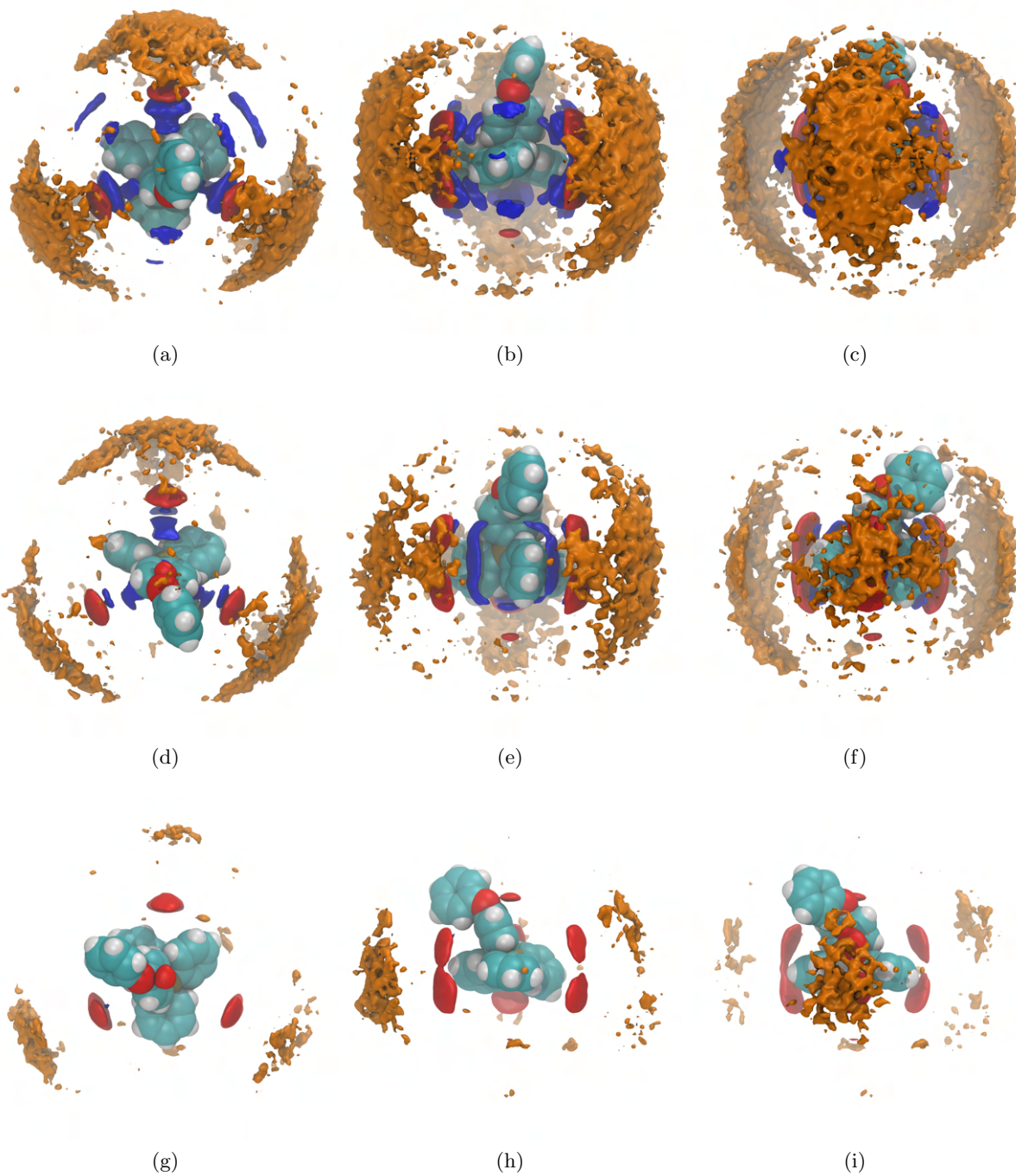


Figure S12: Spatial distribution functions around cations with (a-c) bromobenzene, (d-f) cyanobenzene, and (g-i) perfluorobenzene showing (red,  $3\times$ ) the nitrogen of the anion, (blue,  $3\times$ ) center of mass of neighboring solutes, and (orange,  $1\times$ ) the phosphorous atom of neighboring cations. Left, middle, and right figures show top-down views, front views, and side views, respectively.

## 5 Common Neighbour Analysis

Distance cutoffs used to determine the nearest neighbours for the IL–hydrocarbon systems are provided in Table S2.

Table S2: Distance cutoffs used to determine the nearest neighbours for the IL–hydrocarbon systems.

Pair	TOL	NAP	ETB	HFB	BRB	CYB	MXY	OXY	PXY
HC-ANI	10	10	10	9	10	10	10	10	10
ANI-CAT	11.55	11.55	11.55	11.55	11.55	11.55	11.55	11.55	11.55
HC-CAT	10	10	10	9	10	10	10	10	10
HC-HC	9	9	9	9	9	9	9	9	9

A detailed view of the hexafluorobenzene–IL system as a bicontinuous phase is provided in Figure S13.

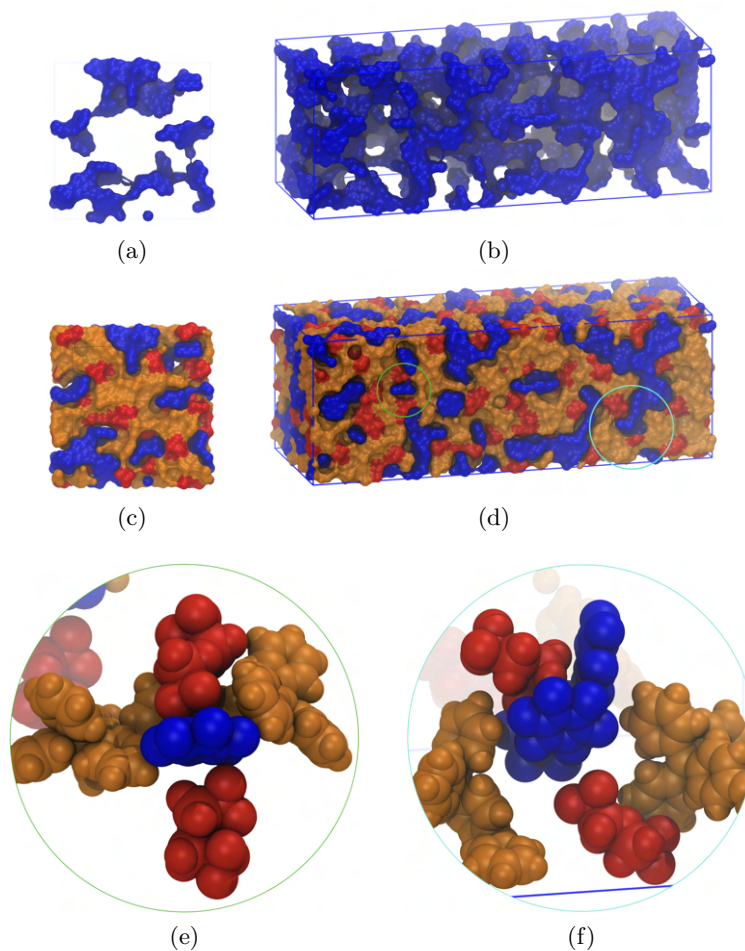


Figure S13: (a,b) Front and side faces of the hexafluorobenzene–IL simulation box showing the connectivity of the toluene phase, in blue. (c,d) Front and side faces of the same simulation box showing the connectivity of the hexafluorobenzene phase and, separately, the cation and anion phase, orange and red, respectively. Circled regions in (d) are expanded to show local molecular arrangements in subfigures (e) and (f).



Heat maps for the different system showing the probability of a simultaneous number of cations and anions around a hydrocarbon are provide in Figure S14.

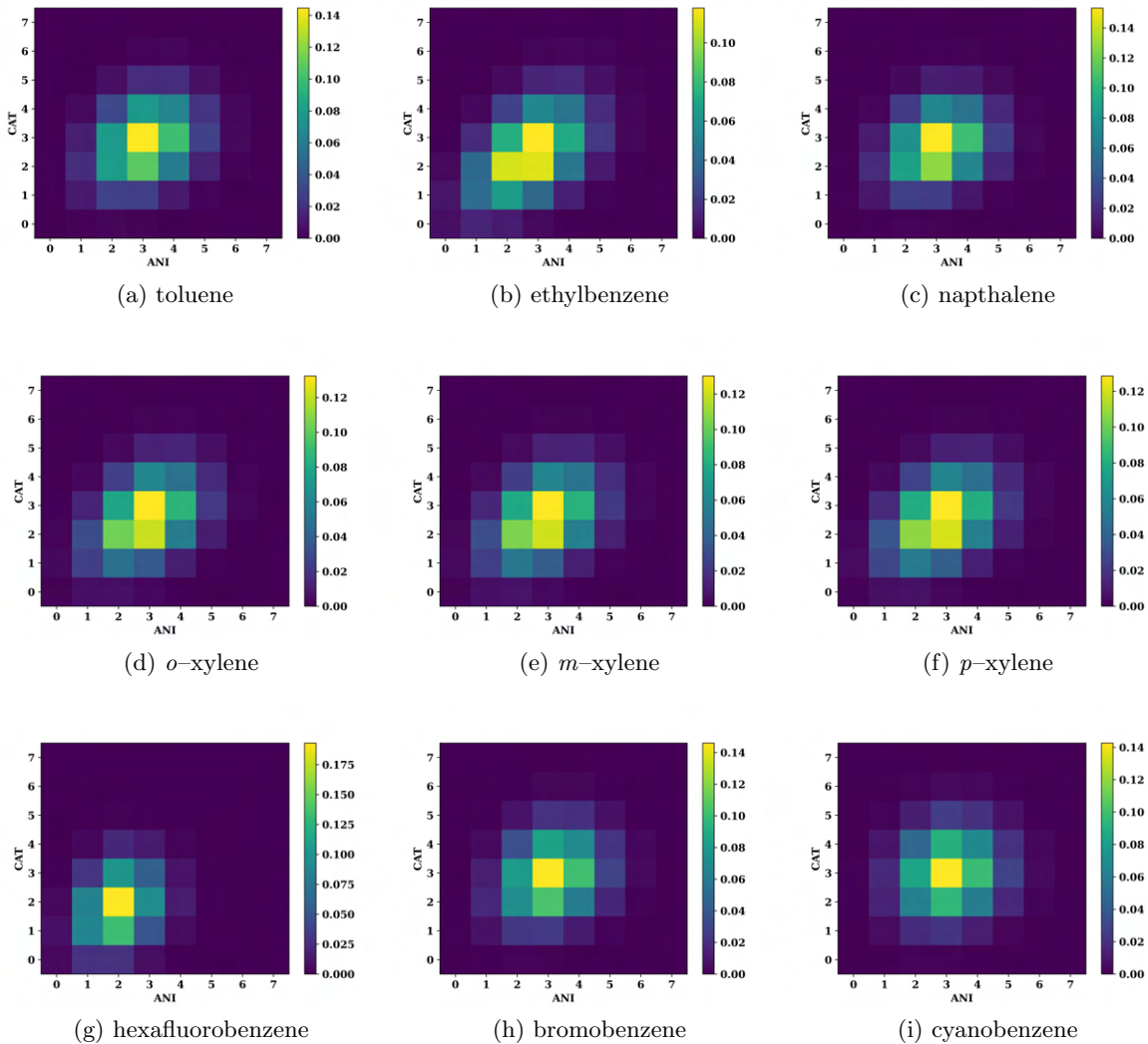


Figure S14: Heat maps for the different system showing the probability of a simultaneous number of cations and anions around a hydrocarbon.

Heat maps for the different system showing the probability of a simultaneous number of anions and toluenes around a cation are provide in Figure S15.

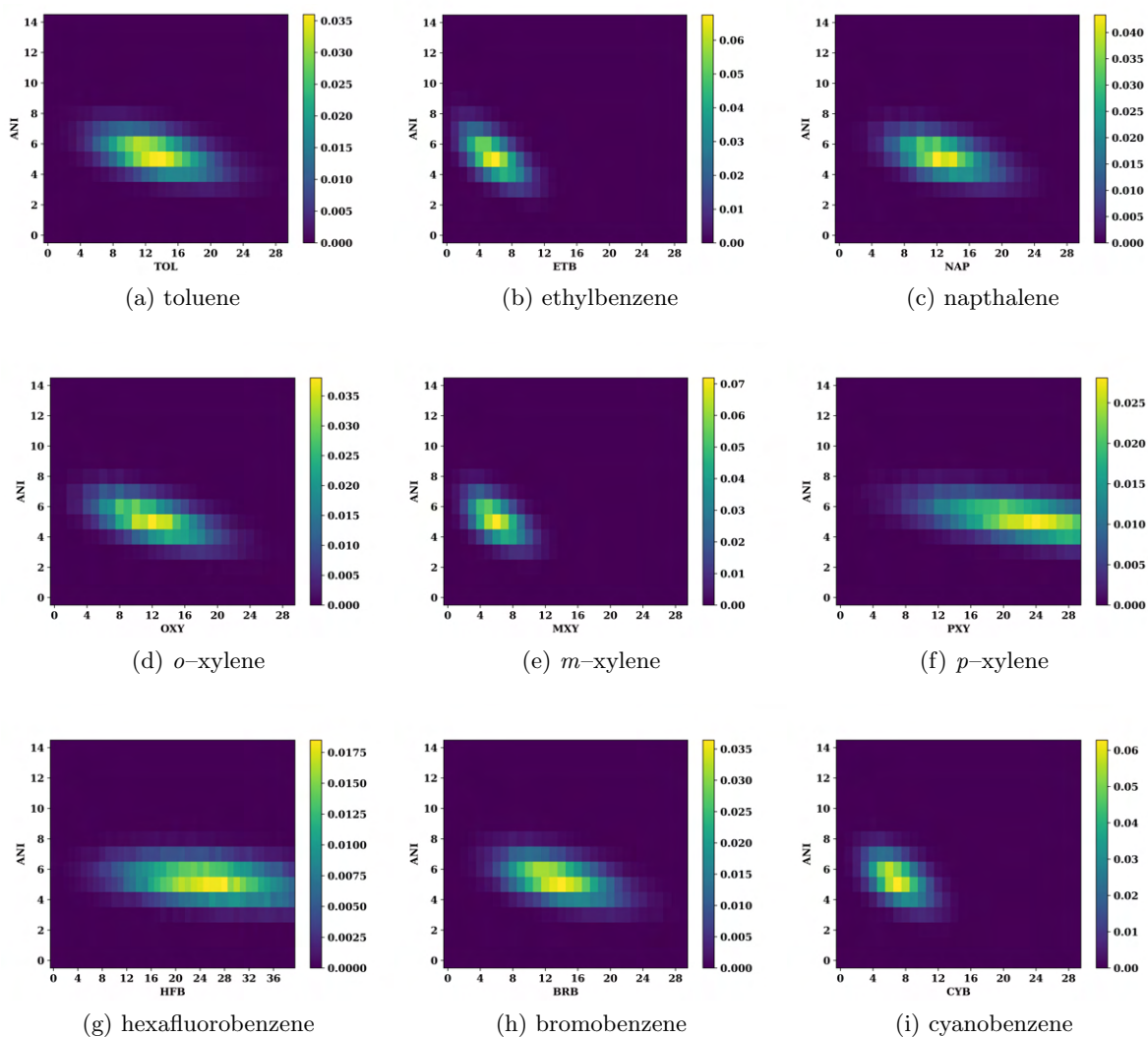


Figure S15: Heat maps for the different system showing the probability of a simultaneous number of anions and toluenes around a cation.

Heat maps for the different system showing the probability of a simultaneous number of cations and toluenes around an anion are provided in Figure S16.

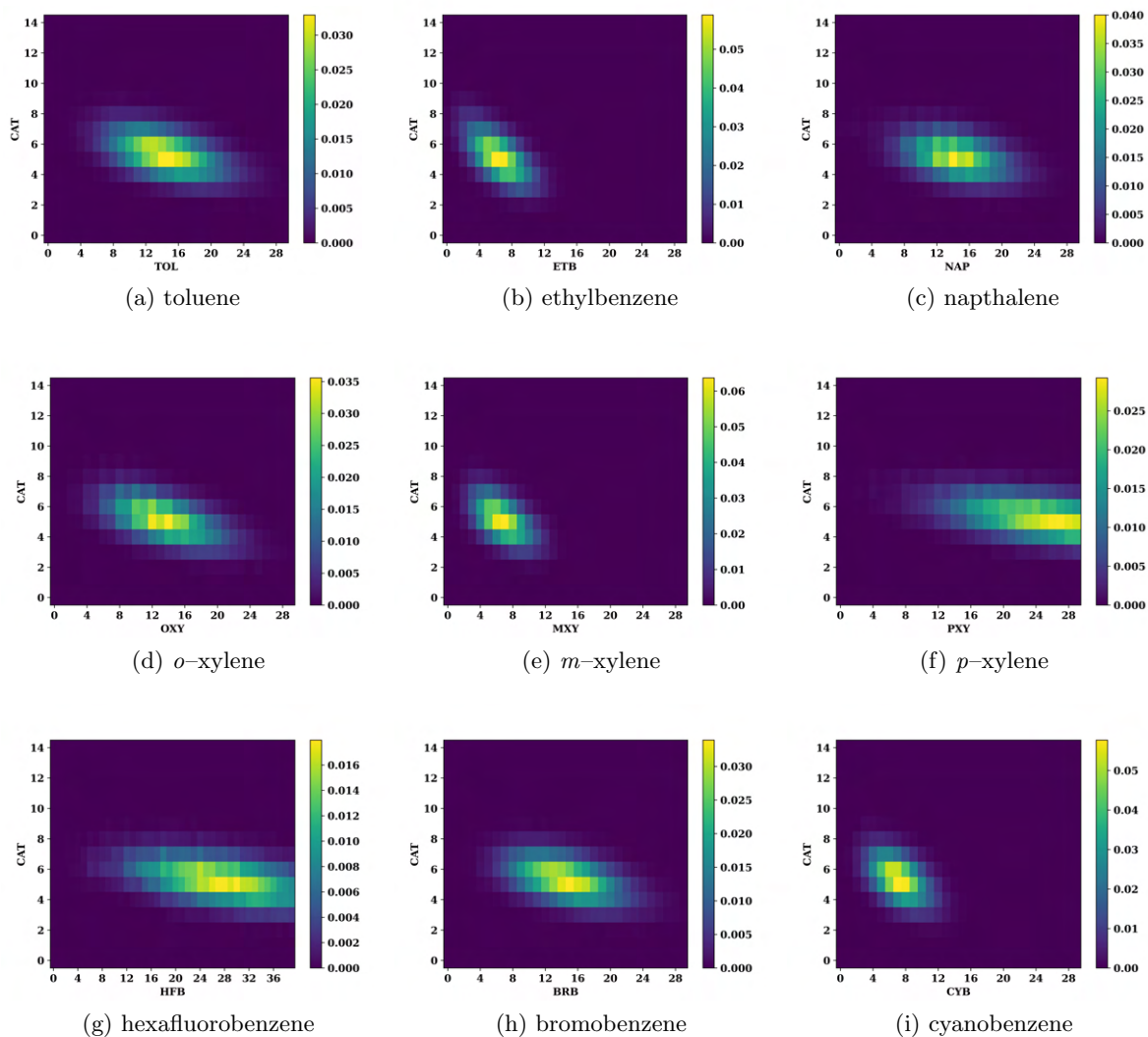


Figure S16: Heat maps for the different system showing the probability of a simultaneous number of cations and toluenes around an anion.

## 6 Connectivity Analysis

Representative images showing the connectivity of the hydrocarbon-hydrocarbon and IL-IL networks are provided in Figures S17 and Figure S18.

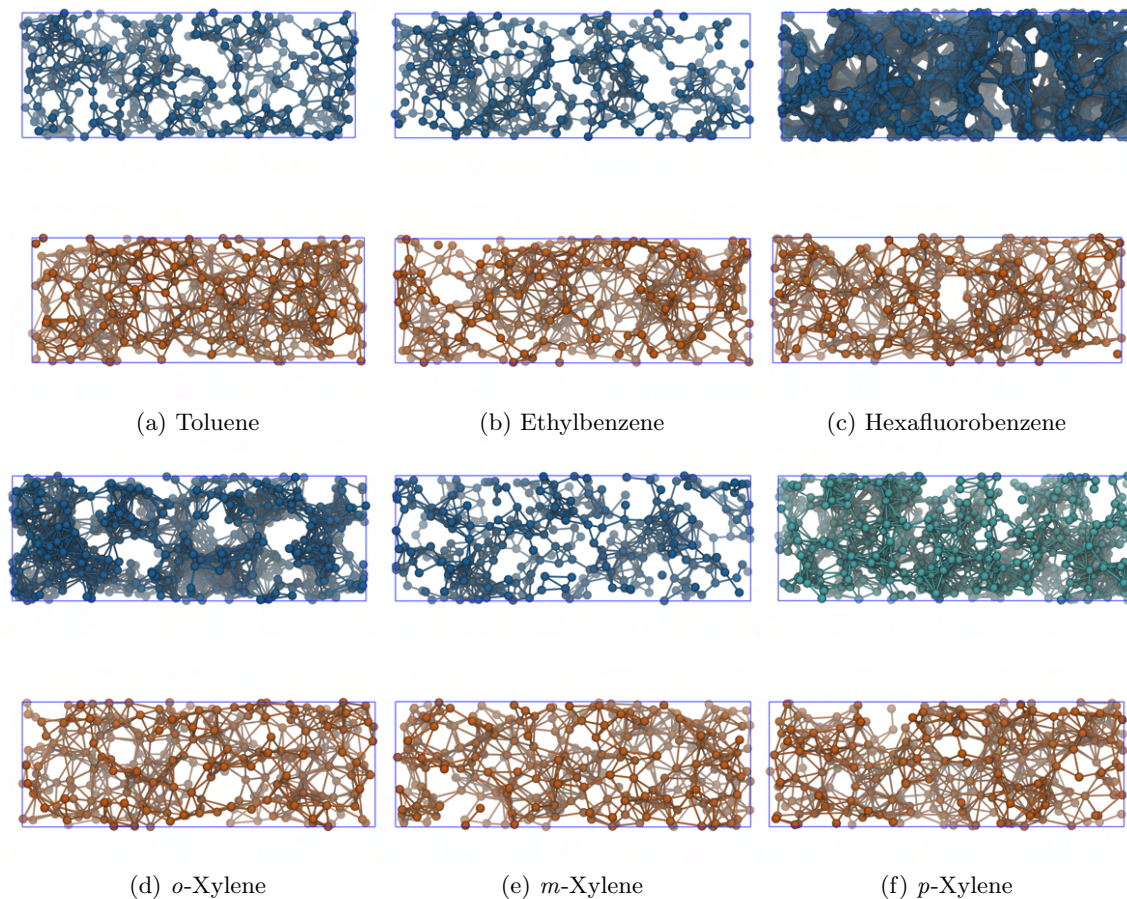


Figure S17: Connectivity of (top of each subfigure, blue) the hydrocarbon-hydrocarbon networks and (bottom of each subfigure, orange) the IL-IL networks for each of the aromatic hydrocarbon systems. Each system shows the same snapshot. Cutoff distances for connectivity are provided in Table S2. The hydrocarbon-hydrocarbon figures display the atom nearest the center of mass and lines between the atoms indicate that the distance between those atoms meets the cutoff criteria. The IL-IL subfigures display the phosphorous and nitrogen atoms of the cation and anion, respectively.

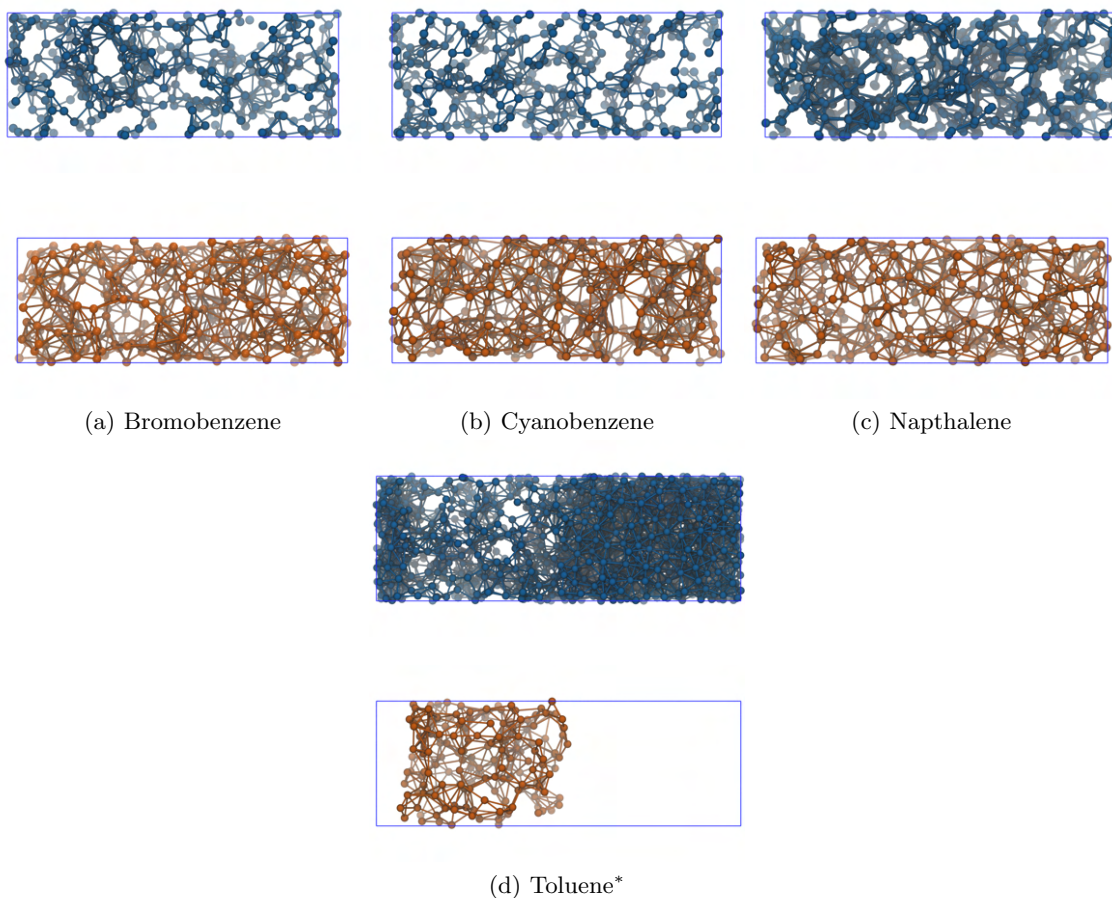


Figure S18: Connectivity of (top of each subfigure, blue) the hydrocarbon-hydrocarbon networks and (bottom of each subfigure, orange) the IL-IL networks for each of the aromatic hydrocarbon systems. Each system shows the same snapshot. Cutoff distances for connectivity are provided in Table S2. The hydrocarbon-hydrocarbon figures display the atom nearest the center of mass and lines between the atoms indicate that the distance between those atoms meets the cutoff criteria. The IL-IL subfigures display the phosphorous and nitrogen atoms of the cation and anion, respectively. The toluene simulation marked with an asterisk indicates the simulation from the Model Validation section of the manuscript.

## 7 Interaction Energies

The standard deviation and standard uncertainties of the calculated pairwise interaction energies for each system are provided in Table S3 and Table S4, respectively.

Table S3: Detailed breakdown of the standard deviation of the change in the pairwise interactions upon mixing, given in kcal/mol.

System	$\Delta U_{CAT-CAT}$		$\Delta U_{CAT-ANI}$		$\Delta U_{ANI-ANI}$		$\Delta U_{CAT-HC}$		$\Delta U_{ANI-HC}$		$\Delta U_{HC-HC}$	
	vdW	Elec.	vdW	Elec.	vdW	Elec.	vdW	Elec.	vdW	Elec.	vdW	Elec.
Toluene	0.10	3	0.08	7	0.02	4	0.51	0.04	0.15	0.04	0.26	0.02
Ethylbenzene	0.004	2	0.03	4	0.005	2	0.22	0.02	0.05	0.02	0.19	0.013
<i>o</i> -Xylene	0.04	4	0.08	8	0.004	4	0.25	0.02	0.10	0.03	0.16	0.011
<i>m</i> -Xylene	0.009	2	0.03	5	0.008	3	0.12	0.03	0.06	0.013	0.12	0.010
<i>p</i> -Xylene	0.06	4	0.06	8	0.007	4	0.30	0.04	0.10	0.011	0.18	0.003
Hexafluorobenzene	0.003	3	0.02	6	0.007	3	0.31	0.013	0.15	0.04	0.24	0.02
Bromobenzene	0.15	0.03	0.10	0.2	0.04	0.10	0.16	0.02	0.08	0.03	0.08	0.008
Cyanobenzene	0.10	4	0.10	9	0.012	4	0.66	0.28	0.21	0.44	0.38	0.11
Napthalene	0.05	3	0.02	7	0.002	3	0.37	0.05	0.09	0.06	0.18	0.010

Table S4: Detailed breakdown of the standard uncertainty of the change in the pairwise interactions upon mixing, given in kcal/mol.

System	$\Delta U_{CAT-CAT}$		$\Delta U_{CAT-ANI}$		$\Delta U_{ANI-ANI}$		$\Delta U_{CAT-HC}$		$\Delta U_{ANI-HC}$		$\Delta U_{HC-HC}$	
	vdW	Elec.	vdW	Elec.	vdW	Elec.	vdW	Elec.	vdW	Elec.	vdW	Elec.
Toluene	0.007	0.2	0.006	0.5	0.0013	0.2	0.04	0.003	0.011	0.003	0.02	0.0015
Ethylbenzene	0.0003	0.2	0.002	0.3	0.0003	0.2	0.02	0.0014	0.004	0.002	0.014	0.0009
<i>o</i> -Xylene	0.003	0.3	0.006	0.6	0.0003	0.3	0.02	0.0014	0.007	0.002	0.011	0.0008
<i>m</i> -Xylene	0.0006	0.2	0.002	0.4	0.0006	0.2	0.009	0.002	0.004	0.0010	0.008	0.0007
<i>p</i> -Xylene	0.004	0.3	0.004	0.6	0.0005	0.3	0.02	0.003	0.007	0.0008	0.013	0.0002
Hexafluorobenzene	0.0002	0.2	0.0013	0.4	0.0005	0.2	0.02	0.0009	0.010	0.003	0.02	0.0011
Bromobenzene	0.011	0.002	0.007	0.012	0.003	0.007	0.011	0.0014	0.006	0.002	0.006	0.0006
Cyanobenzene	0.007	0.3	0.007	0.6	0.0009	0.3	0.05	0.020	0.015	0.031	0.03	0.008
Napthalene	0.003	0.2	0.0015	0.5	0.0001	0.2	0.03	0.003	0.007	0.004	0.013	0.0007